



## Trace detection and discrimination of explosives using electrochemical potentiometric gas sensors

Praveen K. Sekhar<sup>a,\*</sup>, Eric. L. Brosha<sup>a</sup>, Rangachary Mukundan<sup>a</sup>, Kevin L. Linker<sup>b</sup>, Charles Brusseau<sup>b</sup>, Fernando H. Garzon<sup>a</sup>

<sup>a</sup> Los Alamos National Laboratory (LANL), Sensors and Electrochemical Devices Group, Los Alamos, NM 87545, USA

<sup>b</sup> Contraband Detection Technologies, Sandia National Laboratories, Albuquerque, NM 87185, USA

### ARTICLE INFO

#### Article history:

Received 16 November 2010  
Received in revised form 2 March 2011  
Accepted 3 March 2011  
Available online 9 March 2011

#### Keywords:

Explosives detection  
Electrochemical gas sensor  
Mixed potential  
Explosives discrimination  
Low cost sensor technology

### ABSTRACT

In this article, selective and sensitive detection of trace amounts of pentaerythritol tetranitrate (PETN), 2,4,6-trinitrotoluene (TNT) and cyclotrimethylenetrinitramine (RDX) is demonstrated. The screening system is based on a sampling/concentrator front end and electrochemical potentiometric gas sensors as the detector. Preferential hydrocarbon and nitrogen oxide(s) mixed potential sensors based on lanthanum strontium chromite and Pt electrodes with yttria stabilized zirconia (YSZ) solid electrolyte were used to capture the signature of the explosives. Quantitative measurements based on hydrocarbon and nitrogen oxide sensor responses indicated that the detector sensitivity scaled proportionally with the mass of the explosives (1–3 µg). Moreover, the results showed that PETN, TNT, and RDX samples could be discriminated from each other by calculating the ratio of nitrogen oxides to hydrocarbon integrated area under the peak. Further, the use of front-end technology to collect and concentrate the high explosive (HE) vapors make intrinsically low vapor pressure of the HE less of an obstacle for detection while ensuring higher sensitivity levels. In addition, the ability to use multiple sensors each tuned to basic chemical structures (e.g., nitro, amino, peroxide, and hydrocarbon groups) in HE materials will permit the construction of low-cost detector systems for screening a wide spectrum of explosives with lower false positives than present-day technologies.

© 2011 Elsevier B.V. All rights reserved.

### 1. Introduction

The Intelligence Reform and Terrorism Prevention Act of 2004 (P.L. 108-458) directed the Department of Homeland Security (DHS) to place high priority on developing and deploying passenger explosives screening equipment [1]. The recent cargo bomb plot (30 October 2010) using pentaerythritol tetranitrate (PETN) and/or triacetone triperoxide (TATP) for sabotage has initiated an urgent and compelling need to reliably detect bulk and trace amount of explosives in a cost-effective way. Further, the Christmas Day bombing plot (25 December 2009) using PETN has exposed weaknesses in the current system of explosives detection.

The focus of this article is on trace detection of explosives. Trace detection looks for residue or contamination from handling or being near explosive materials. Detection of trace contamination can, however, expose a bulk source. Reviewing the techniques for trace detection of explosives [2–4], ion mobility spectrometry (IMS) appears to possess the required sensitivity in field-testing. Though IMS systems have advantages of simplicity, small size, and

short response time, their ability to sense only electronegative compounds (for example, nitro groups), false positive susceptibility, and sensitivity to changes in ambient conditions have rendered them less versatile against a wide pool of explosives [5]. Such characteristics preclude the use of IMS in the analysis of those explosives containing organic peroxides and amine groups. For example, TATP and hexamethylenetriperoxydiamine (HMTD) have become increasingly popular among terrorists due to the ease of manufacturing and readily available starting materials [6]. Further, the list of explosives [7] furnished by the Bureau of Alcohol, Tobacco, Firearms, and Explosives (BATF) indicates that an IMS can detect a very minimal subset of the ever-expanding roll of high-energy explosives. Hence, there is an immediate need for an explosives detection technology that can screen a wide array of explosives containing different functional groups at low cost.

Chemical sensors, as an alternate detection strategy, have the potential [8] to mimic the canine system, which is known to be the most reliable and mobile method for detecting a wide range of suspicious substances. In many chemical sensor systems, a receptor layer is used to bind the target explosives of interest upon which a change in physical or chemical parameters is triggered. Ample open literature exists on trace detection of explosives with different transduction principles [9–12]. For example, Caron et al. [13]

\* Corresponding author. Tel.: +1 505 665 8996.

E-mail address: [psekhar@lanl.gov](mailto:psekhar@lanl.gov) (P.K. Sekhar).

described a system for the detection of nitroaromatic explosives consisting of a portable detector based on a specific fluorescent material—a diimine phenylene–ethynylene compound.

In the presence of nitroaromatic vapors such as trinitrotoluene or its derivative 2,4-dinitrotoluene (DNT), the fluorescence of the material was found to decrease due to the adsorption of nitroaromatic molecules on its specific adsorption sites. On the other hand, Larsson et al. [14] investigated two types of thiols that are self-assembled to produce a biochip on gold, namely oligo (OEG)-alkyl thiols terminated with a hydroxyl group and a TNT-analogue (2,4-dinitrobenzene), respectively. Surface plasmon resonance (SPR) and quartz crystal microbalance (QCM) techniques were used to monitor the dissociation of immobilized monoclonal antibodies produced against TNT. A common area of concern for many of the investigators is the challenge of discriminating the explosives.

Among the several classes of chemical sensors, electrochemical systems [15,16] impart high selectivity, portability, a wide linear range, minimal space and power requirements combined with the ability to lower the deployment cost of sensors using mass production. The drawback of electrochemical devices is the poor sensitivity in detecting explosives vapor, as the vapor pressure of most explosives is extremely low. However, the presence of a preconcentrator addresses the above problem. The role of a preconcentrator is to take a trace sample of an explosive (or other material to be studied) from a large incoming airflow and concentrate the material into a much smaller volume before it is introduced into a trace detector. Sandia National Laboratories (SNL) has developed and patented [17,18] a state-of-the-art preconcentrator system (a hand-portable sample collection and preconcentrator device), which, when combined with a sensor unit, is capable of detecting vanishingly faint odors (parts per trillion) of explosives, drugs, and other chemicals. Leveraging such an engineered system, amperometric [19] and potentiometric sensing [20,21] for trace detection of explosives has been reported. Cizek et al. [19] reported amperometric detection of TNT because nitroaromatic compounds such as TNT are readily reduced at mercury and carbon electrodes, allowing their electrochemical determination. The reduction peaks resulting from the step-wise reduction of TNT to the corresponding hydroxylamine and amine compounds enabled its quantitative detection. According to the authors, linear signal dependence was observed between the measured current and the concentration of TNT (0.25–10  $\mu\text{g}$ ). The detection mechanism reported in this investigation only focuses on redox nitro groups and did not furnish any details on the potential for this sensor to discriminate explosives.

Alternatively, non-Nernstian potentiometric gas sensors have shown promising selectivity for the detection of exhaust gases such as hydrocarbons (HCs), oxides of nitrogen ( $\text{NO}_x$ ),  $\text{NH}_3$ , and CO [22–24].

The sensors group at Los Alamos National Laboratory (LANL) has developed mixed potential sensors for detecting  $\text{NO}_x$ , CO, and HCs [25–27]. Mixed potential sensors are a class of electrochemical devices that develop a non-Nernstian electromotive force (e.m.f) due to the difference in the kinetics of the redox reactions at each electrode/electrolyte interface upon exposure to various analytes [28]. These sensors rely on the fact that two dissimilar electrodes along with an oxygen-ion conducting electrolyte exhibit different non-equilibrium potentials in the presence of a reducing gas and oxygen. The LANL mixed potential sensor design is unique and possesses several inherent advantages [29–31]. Two of the characteristic features leading to exceptional stability and sensitivity were the minimized electrode–electrolyte interface and stable three-phase interface by materials selection and design. The sensor design used dense electrodes and a porous electrolyte, unlike conventional oxygen sensors. Further, the material selection for the electrodes typically involved one electrode with fast (Pt, lanthanum strontium manganite) and another with slow (Au, indium

tin oxide, lanthanum strontium chromite)  $\text{O}_2$  reduction kinetics aimed at improving the sensitivity).

In this article, trace detection of high explosives (HE) using mixed potential gas sensors in combination with established front-end technology is demonstrated. HC and  $\text{NO}_x$  sensor response is used to capture the signature of the explosives. Further, the discrimination of explosives such as PETN, TNT, and RDX is shown.

## 2. Experimental

### 2.1. Sensor preparation and testing

First, the mixed potential sensors were prepared, tested for different gases, and optimized for their hydrocarbon and  $\text{NO}_x$  response. The sensors consist of a  $\text{La}_{1-x}\text{Sr}_x\text{CrO}_3$  (LSCrO) working electrode, a Pt counter-electrode and YSZ (oxygen ion conductor) electrolyte. LSCrO pellet electrodes of different compositions ( $x = 0.1, 0.2, 0.3$ ) were prepared from their respective powder versions procured from Praxair®. The powders were first uniaxially pressed in a 1.9 cm die at 15 MPa for 5 min and then isostatically pressed at 200 MPa for 5 min. Then, the LSCrO samples were sintered at 1650 °C for 10 h and box-rectangle shaped slices with dimensions approximately 0.1 cm  $\times$  0.02 cm  $\times$  0.01 cm were cut from this ceramic piece using a wet diamond saw. These small, ceramic LSCrO bars served as the working electrode for the sensor.

The prefabricated LSCrO electrode along with a Pt wire (dia. = 0.025 cm) were then partially embedded between two wet layers of YSZ tape to form a green sensor. Once dry, the excess YSZ with plasticizers and sintering aids is trimmed away to minimize the overall size of the sensor. The green body forming the sensor is then heated to sinter the electrolyte tape around the electrodes to achieve mechanical stability and the prerequisite ionic conductivity between the two electrodes. More details on the tape-casting process can be found elsewhere [32]. The sensor configuration is shown in Supplementary data Fig. S1. After fabricating the sensor, it was mounted on an alumina rod with Pt leads, which was then placed in a quartz tube and heated in a furnace to the desired operating temperature (500 °C).  $\text{NO}$ ,  $\text{NO}_2$ ,  $\text{NH}_3$ ,  $\text{C}_3\text{H}_6$ , and CO were used as test gases, each with a concentration of 100 ppm. The flow rates of the various gas mixtures were controlled using analog MKS-brand mass flow controllers, while the voltage from the sensor was monitored using a Keithley 2400 Source Measure Unit (SMU) with the Pt electrode connected to its positive terminal. The flow rate of the mix gas was adjusted so as to give the appropriate concentration of the sensing gas in the test mixture. Air was used as the base gas (partial pressure of oxygen: 21%). The total flow rate was maintained at 200 sccm. Among the sensors tested, two devices were selected to detect explosives based on higher sensitivity levels to hydrocarbons and  $\text{NO}_x$  with minimal interference to other gases. The HC and  $\text{NO}_x$  sensor response is shown in Supplementary data Fig. S2.

### 2.2. Explosives screening

Trace samples of common military high explosives samples were obtained using Accustandards™ (high purity analytical calibration standards typically used to calibrate IMS and gas chromatography/mass spectroscopy (GC/MS) analytical instrumentation). The total volume of the samples procured was 1 mL. PETN (99.8  $\mu\text{g}/\text{mL}$ , balance methanol), TNT (1000  $\mu\text{g}/\text{mL}$ , balance 1:1 acetonitrile and methanol solvent), and RDX (995  $\mu\text{g}/\text{mL}$ , balance 1:1 acetonitrile and methanol solvent) formed the *de minimus* quantities of explosives. The HE/solvent sample was transferred onto a NiCr wire using a micropipette. The hotwire had a thermocouple spot-welded to it to monitor the temperature. It should

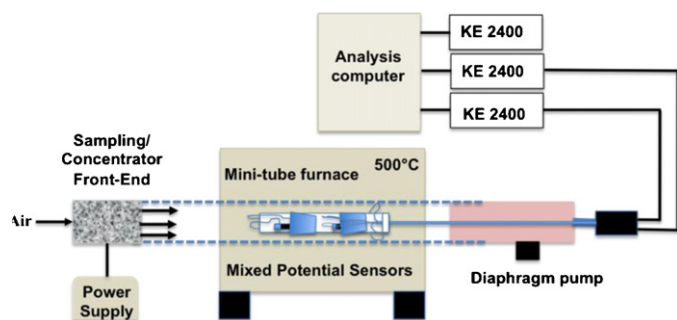


Fig. 1. Experimental setup for the detection of explosives.

be noted that the function of the hot wire is for sample loading and transfer of the explosive vapor onto the felt. For field-testing applications, the hot wire is not needed. The evaporation of the solvent from the hot wire was identified easily by monitoring the temperature of the hot wire.

After evaporation of the organic solvent, the hot wire was rapidly heated (to temperatures less than the decomposition temperature of the explosives) using a succession of four pulses separated by pauses of 8–9 s. This procedure increased the vapor pressure of the sample sufficiently to desorb the HE molecules from the hotwire surface. The sampling/concentrator front-end unit was positioned approx. 2.5 cm away from the hot wire. This device collected and concentrated the HE sample and is comprised of essentially a high-surface-area stainless steel felt.

The sampling unit pulled a stream of room air through a high-speed motor with impeller (volume of flow ca. 11,326,738.4 cm<sup>3</sup>/min) and subsequently the HE vapor and particulates of HE were trapped on the surface of the felt [17]. After trapping the HE molecules on the surface of the felt, the collector felt module was rapidly heated with high degree of reproducibility (<1 s) to the desired set-point temperature (185 °C, 170 °C, and 190 °C for PETN, TNT, and RDX respectively) in airflow (200 cc/min). The rapid heating of the collector felt results in the release of HE molecules from the felt surface (they were adsorbed to) directly to LANL mixed potential gas sensors operating downstream in a miniature tube furnace at 500 °C.

Of the two sensors inside the furnace, one was tuned for preferential NO<sub>x</sub> response by the appropriate application of a current bias [33] and the other for HC response under open-circuit conditions. A current bias of 0.1 μA was applied to the NO<sub>x</sub> sensor. The operating temperature of the sensors had to be compromised as the NO<sub>x</sub> sensor had superior selectivity at 500 °C while the hydrocarbon sensor was subjected to below-optimized performance conditions. As a part of future research, a cold wall setup utilizing sensors with integrated heaters for independent control of sensor temperature is envisioned to circumvent this problem.

First, the background signal in the absence of explosives vapor was collected for both the sensors by flashing the felt without the trace explosives adsorbed on them. Further, the concentrations of the explosives were varied (1, 2, and 3 μg) to observe the sensor response. The area under the peak for the HC and NO<sub>x</sub> sensor is an indicator of the device sensitivity.

### 3. Results and discussion

Fig. 1 shows the experimental setup for trace detection of explosives with SNL sampling/concentrator unit as the front end and the mixed potential gas sensors housed in a mini tube-furnace (0.5 in. tube dia.) as the detector.

The sensor leads were connected to the 2400 Keithley source meters to monitor the HC and NO<sub>x</sub> response while the temperature of the surface in contact with the HE samples was recorded through

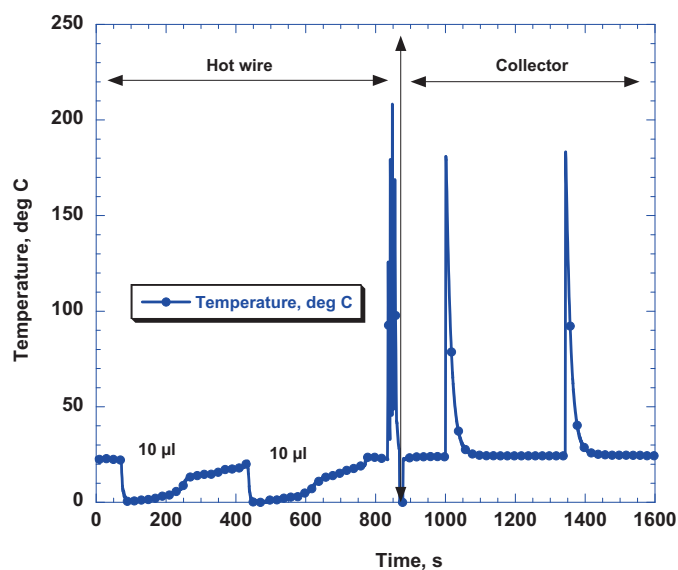
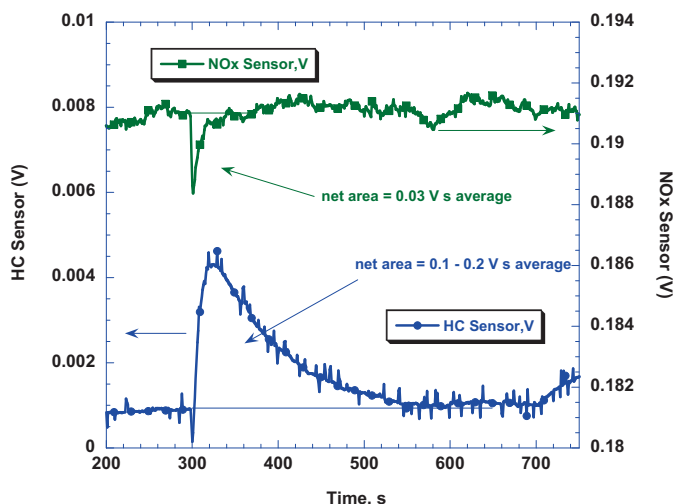


Fig. 2. Temperature profile of the hot wire and collector during a 2 μg, 2 × 10 μL PETN dispense.

another 2400 Keithley source meter via a Fluke 80TK thermocouple module. Fig. 2 illustrates the temperature profile of the hot wire and the collector felt during a test sequence with 20 μL (2 μg) of PETN as the analyte. As the size of the hotwire was unable to handle liquid volumes larger than 10 μL, a 2–10 μL dispensing sequence was adopted without losing any portion of the droplet.

As seen from Fig. 2, a significant drop in temperature was observed when the sample was loaded onto the hot wire, indicating the evaporation of solvent with the hot wire returned to room temperature after all the solvent evaporated. In the temperature profile, the hot wire part and the collector felt part are clearly demarcated as the thermocouple module is first used to monitor the temperature of the hot wire, then grounded, and switched back to monitor the temperature of the collector felt. Between 800 and 900 s in the hot wire portion of the temperature profile, four pulses resulting in temperature spikes averaging 185 °C can be seen. It should be noted that there is a possibility of a minute quantity of explosive disintegration on the hotwire if the hotwire temperature exceeded the decomposition temperature of the analyte. The transfer of explosive sample from the hot-wire to the collector felt would need to be optimized for each type of high explosive to insure the generation of optimum calibration curves from the sensors for a given mass of explosive sample. At present, such an effect simply lowers the available explosive vapor for sensing and otherwise would have little effect on detector sensitivity if minimized. The analyte vapor was transferred to the collector felt. Between 900 and 1000 s, the collector felt with adsorbed HE molecules is locked into a placeholder (clamping force applied using a cam such that the air flow goes through the sample/collector felt and onto the sensors), which is connected to the opening of the mini-tube furnace through customized transfer tubes. As expected, the sensors did not respond to just the placement of the collector felt. There was no disruption or disturbance in the baseline response of the sensor. This was a clear indication that the HE sample remained adsorbed onto the surface of the felt at room temperature. The sensor responded only when the collector felt was flashed at 185 °C (at 1000 and 1390 s from Fig. 2). The applied heat rapidly desorbed the HE sample from the collector felt.

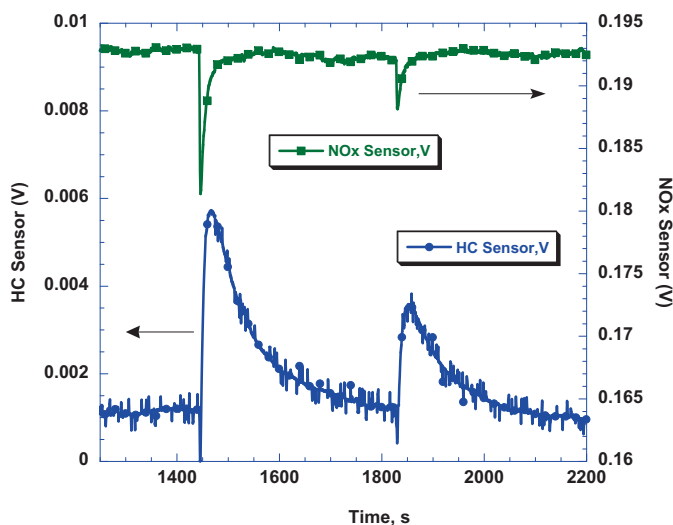
Before recording the sensor response due to the PETN sample, a baseline signature was collected without the explosive adsorbed on the felt. The collector felt was placed on the placeholder without an explosive trace and flashed at 185 °C.



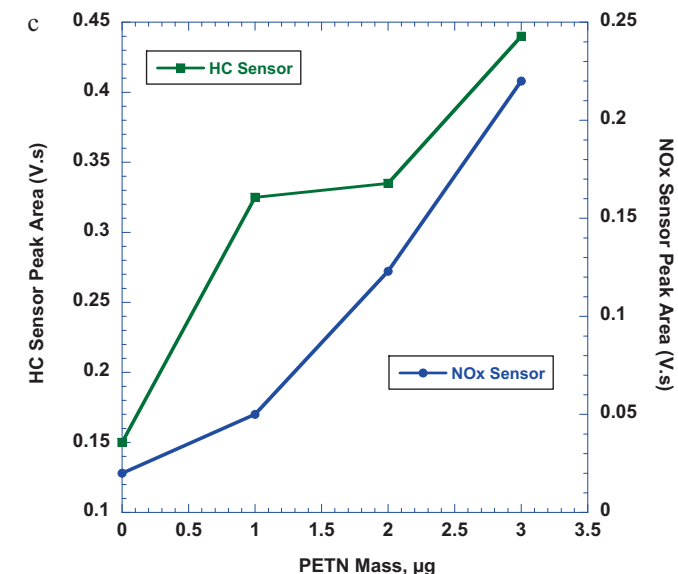
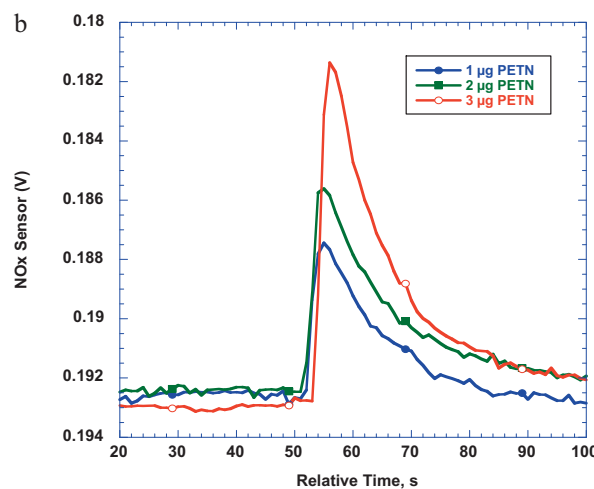
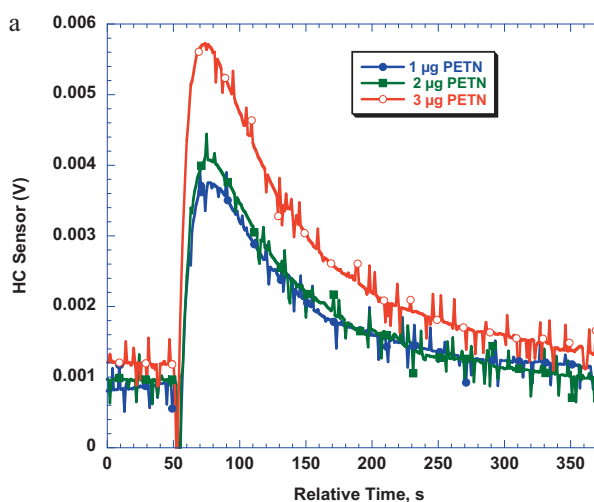
**Fig. 3.** Baseline HC and  $\text{NO}_x$  response after flashing collector felt to  $185^\circ\text{C}$ . Flowing room air: 200 cc/min.  $\text{NO}_x$  sensor biased at 0.0001 mA. Integrated peak areas are indicated.

Fig. 3 shows the baseline response of the HC and  $\text{NO}_x$  sensor upon flashing the “empty” or “clean” felt. Both the HC and  $\text{NO}_x$  sensor deviated from their sensor baselines with minor perturbations, and the origin of this response is still under investigation. At this point, the anomalous baseline response is attributed to outgassing of the insulation on thermocouple wire that was attached to the surface of collector felt. The average area under the peak for the HC and  $\text{NO}_x$  baseline response was found to be 0.15 V s and 0.03 V s, respectively. Then, the collector felt with PETN vapor/molecules was flashed. Fig. 4 shows the HC and  $\text{NO}_x$  response corresponding to  $3\ \mu\text{g}$  of PETN. The sensor signal due to the first flash was much stronger than the second flash, indicating the transfer of vapor from the collector felt to the sensors had occurred. On the other hand, the magnitude of the second flash is seen closer to the baseline response, denoting diminishing vapor content released from the collector felt. It is assumed that all the vapor/gas phase molecules desorb from the collector felt in a single flash at  $185^\circ\text{C}$ . Lowering the felt temperature would result in the need to use multiple flashes to complete the desorption of the HE sample from the felt.

Fig. 5 shows the HC and  $\text{NO}_x$  sensor response as a function of PETN concentration (mass) transferred from the hotwire. With an



**Fig. 4.** HC and  $\text{NO}_x$  response from  $3\ \mu\text{g}$  of PETN after flashing collector felt to  $185^\circ\text{C}$ . Flowing room air: 200 cc/min.  $\text{NO}_x$  sensor biased at 0.0001 mA.



**Fig. 5.** Detector response as a function of PETN mass (200 cc/min,  $500^\circ\text{C}$ ), (a) hydrocarbon response, (b)  $\text{NO}_x$  response, and (c) area under the peak for HC and  $\text{NO}_x$  sensor.

increase in the concentration of PETN, the sensor response seems to augment for both HC and  $\text{NO}_x$  sensor (Fig. 5a and b, respectively). As the baseline response cannot be neglected from the response due to presence of explosives, baseline correction is considered essential prior to calculating the sensor peak areas. Fig. 5c shows

the plot of area under the peak values as a function of PETN mass. As mentioned earlier, the area under the sensor peaks accounts for the sensitivity and not the signal magnitude (or height). While a near linear trend in  $\text{NO}_x$  response was observed with varying concentration (mass) of PETN, the HC response was less so. In the case of HC response behavior, linearity can be assumed if the  $1 \mu\text{g}$  data point is omitted. However, the gas-phase chemistry of the explosive as a function of its concentration cannot be overlooked. Further, the effect of PETN decomposition on the LSCrO, Pt electrodes and YSZ electrolyte is an unsolved problem and demands extensive investigation. The possibility of the HC sensor being piece-wise dependent on PETN concentration cannot be ruled out.

The sensor area for  $0 \mu\text{g}$  of PETN is derived from the baseline response, characterized by the absence of any explosive vapor. Upon exposure to explosive vapor ( $1 \mu\text{g}$  of PETN), a higher HC sensor peak was observed. At  $500^\circ\text{C}$ , PETN decomposes into many gaseous products that include CO.

The developed hydrocarbon sensor for this investigation is cross sensitive to CO. With increase in PETN concentration, it is hypothesized that CO gets oxidized and is displaced from the system resulting in an increase in HC sensitivity. For a better understanding of the relationship between the sensitivity and the concentration of the explosives, it is essential to (a) investigate the gas phase decomposition of the explosives at the operating temperature of the sensors, (b) study homogenous (in the system) and heterogeneous catalysis (on the sensor electrodes and electrolyte) as a function of explosives concentration, and (c) thermodynamics and kinetics of gas phase flow of the explosive vapor over hot surfaces. These critical research tasks form a part of future investigation along with the desire to design a cold wall set-up with integrated heaters on the sensor body.

Similar experimentations were carried out with TNT and RDX. Of the three explosives tested, RDX has the lowest vapor pressure (concentration in air ca.  $10^{-12}$ ). Fig. 6 shows the area under the peak for HC and  $\text{NO}_x$  sensor as a function of RDX mass. It is interesting to note that the shape of the RDX curves (both HC and  $\text{NO}_x$ ) is different from that of PETN indicating the gas-phase chemistry and decomposition kinetics of the explosives plays a critical role in determining the potentiometric behavior of the sensors. Moreover, a non-linear response was observed for the HC and  $\text{NO}_x$  sensor with varying concentrations of RDX. The fact that the behavior of the HC and  $\text{NO}_x$  is different for explosives with varying chemical signature can be seen as a unique feature of this technology leading to selectivity.

Further, the response curves indicate a possibility of detecting trace amounts as low as  $250 \text{ ng}$  of RDX. It is interesting to note that such a detection limit is possible with the current hot-wall setup. In the current setup, the furnace temperature is maintained at  $500^\circ\text{C}$  and a gap of 3 in. exists between the collector felt placeholder to the actual position of the sensors. The vapor travels nearly 3 in. while being exposed to  $500^\circ\text{C}$  (well above the decomposition temperature of the explosives). Inevitably, there is loss of sensitivity due to heterogeneous catalysis and homogeneous decomposition of the vapors before any electrochemical activity at the sensor interface. To improve the limits of detection, a cold-wall setup with integrated heaters on the sensor body is envisioned. From Fig. 6, an increase in the peak area was also observed when the average flash temperature of the hot wire was reduced by  $15^\circ\text{C}$ . It is evident that a minute quantity of explosive disintegrates at higher temperatures (though the hot wire is flashed well below the decomposition temperature of the explosive) during the process of elevating its vapor pressure.

Based on the results, the authors believe that the flash temperature of the hot wire can be optimized for each HE type independent of sensor optimization. Issues of this nature are important for pre-

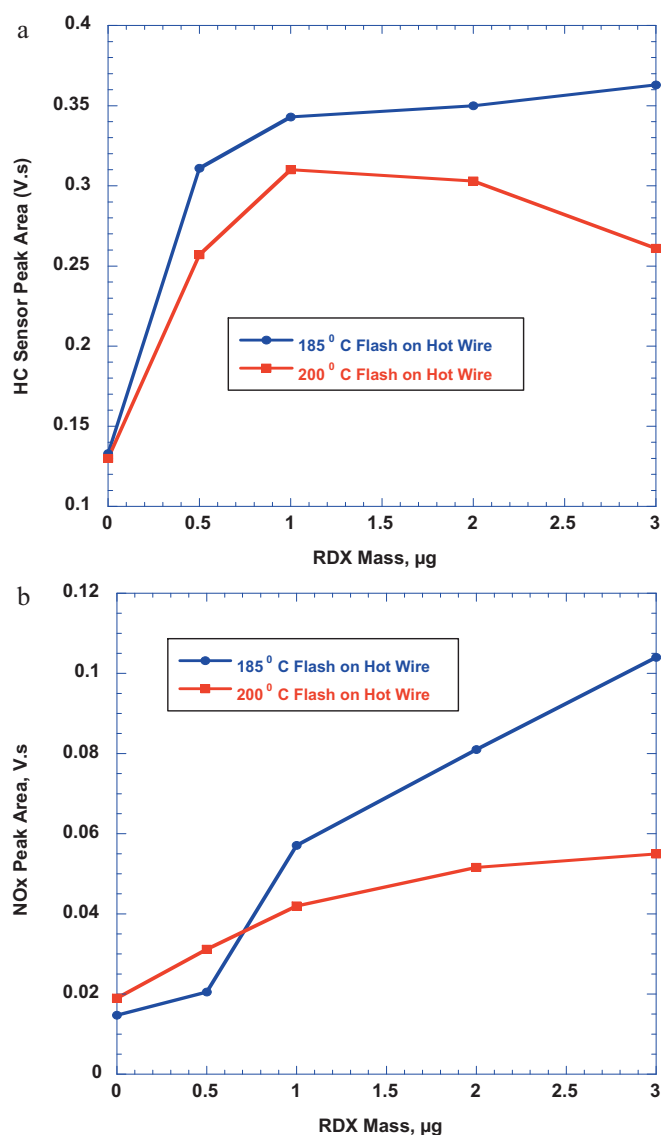


Fig. 6. Area under the peak for RDX as a function of mass. (a) HC response and (b)  $\text{NO}_x$  response.

cise and accurate calibration of the sensors if used in an analytical capacity.

Fig. 7 shows the HC and  $\text{NO}_x$  sensor area for various concentrations (mass) of TNT. A non-linear augment was observed for both HC and  $\text{NO}_x$  sensors peak with an increase in TNT concentration. Fig. 8 compares the HC and  $\text{NO}_x$  response of the baseline, TNT (low vapor pressure,  $10^{-8}$  in air) and RDX (high vapor pressure,  $10^{-12}$  in air). Since the initial source concentration of TNT and RDX were the same, it was relatively easy to prepare a  $10 \mu\text{g}$  sample. The hydrocarbon sensor response exhibited a discernible increase in sensor signal for RDX when compared to TNT. On the other hand, the RDX  $\text{NO}_x$  response recorded a peak area three times greater than that of TNT. It should be noted that the molecular formula for RDX and TNT are  $\text{C}_7\text{H}_5\text{N}_3\text{O}_6$  and  $\text{C}_3\text{H}_6\text{N}_6\text{O}_6$ , respectively.

Based on the stoichiometry, it can be hypothesized that the total  $\text{NO}_x$  generated from the decomposition of RDX would be greater than that of TNT and hence the difference in sensor signatures. It appears as though the HC and  $\text{NO}_x$  sensor response is related to a degree unique to the chemical structure of the explosives (e.g., nitro, amino, peroxide, and hydrocarbon groups). In that context, Table 1 presents a potential discrimination mechanism with three

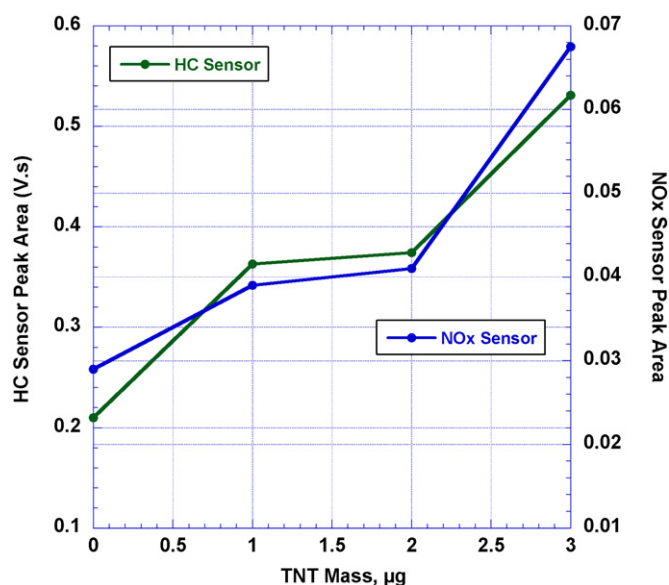


Fig. 7. Area under the peak for hydrocarbon and  $\text{NO}_x$  sensor as a function of TNT mass.

high explosives listed left to right in the order of reducing vapor pressure and decreasing carbon-to- $\text{NO}_x$  ratio. The chemical formula for each explosive has been highlighted so as to quantify the number and nature of the nitro groups. It can be inferred from Table 1 that the ratio of peak area measured by the HC sensor to the peak area measured by the total  $\text{NO}_x$  sensor is unique for each explosive. Such a scheme has the potential to discriminate between the explosives once the gas phase chemistry is understood and the sensor setup optimized to linearize the sensor response with respect to explosive concentration. The measurements recording the HC and  $\text{NO}_x$  sensor response for each explosive were repeated and a statistical variation of  $\pm 2\%$  in the ratio (HC peak area/ $\text{NO}_x$  peak area) was observed.

The fact that a unique ratio of HC/ $\text{NO}_x$  is obtained for each species of HE identifies a method of discriminating high explosives using electrochemical potentiometric gas sensors. The ability to use multiple sensors each tuned to basic chemical structures (e.g., nitro, amino, peroxide, and hydrocarbon groups) constituting the HE will permit the construction of detector systems with an intrinsic ability to lower false positive rates than present-day technologies.

The most fascinating and unique facet of this approach is the prospect of a single detection technology to capture the signature of a wider HE chemistry. Despite the promising results reported in this article, further electrochemical sensor engineering and development will be required in order to realize the potential benefits of this work as it would apply to a new trace explosives detection technology. Some of the potential challenges that need to be addressed include (a) the achievement of required limits of detection (nanogram and possibly sub-nanogram) by transitioning from a hot-wall setup (as used in this work) to a cold-wall setup with integrated heaters on the body of the sensor, (b) transformation

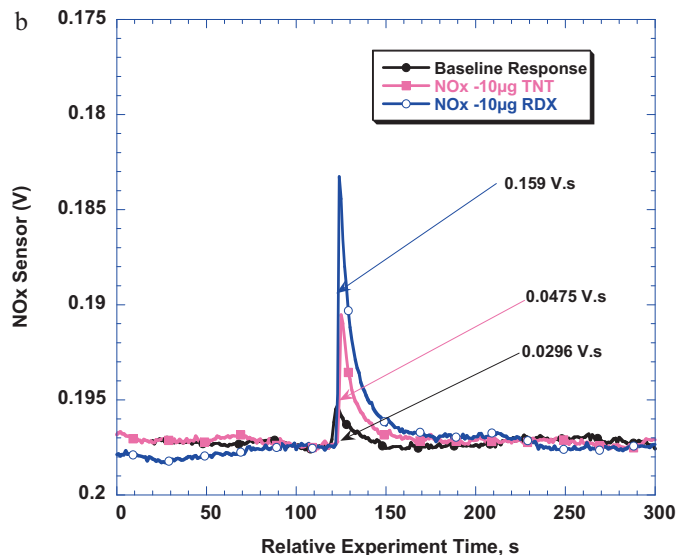
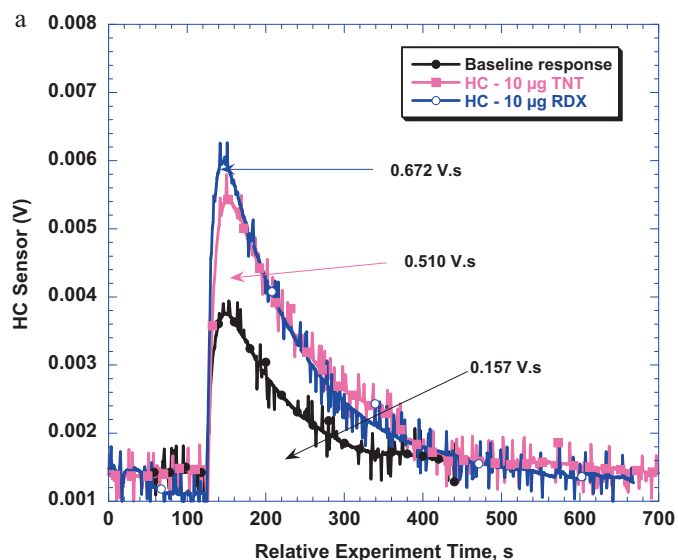


Fig. 8. Comparison of TNT and RDX sensor response (10  $\mu\text{g}$ , 200 mL/min, 165–170 °C flash temperature). (a) Hydrocarbon signature and (b)  $\text{NO}_x$  signature. Integrated peak area is indicated.

of discrete electrochemical sensors used in present work to planar thin-film array configuration by understanding the effect of electrode thickness and dimensions on the sensor performance, and (c) attaining minimal false positives in field trials by deriving a database of potential explosives and non-hazardous substances (for example, food, medicines and cosmetics, a relevant concern for airport deployment).

Moreover, the sensitivity and selectivity levels of the current systems can be significantly enhanced by (a) understanding the

**Table 1**  
Potential explosives discrimination mechanism (ratio of peak area measured by the HC sensor to the peak area measured by the total  $\text{NO}_x$ , 10  $\mu\text{g}$  of all explosives).

Peak area ratio	TNT	PETN	RDX
	$\text{C}_7\text{H}_5(\text{NO}_2)_3$	$\text{C}_5\text{H}_8(\text{NO}_2)_4\text{O}_4$	$\text{C}_3\text{H}_6(\text{NO})_6$
	$\text{C}/\text{NO}_x = 2.30$	$\text{C}/\text{NO}_x = 1.25$	$\text{C}/\text{NO}_x = 0.50$
Felt flash temp. (°C)	170	185	190
HC/ $\text{NO}_x$	10.73	2.13	4.22

gas-phase decomposition chemistry of the explosives [34] through gas chromatography/mass spectroscopy systems attached to the outlet of the furnace, (b) studying the stability and degradation processes of the HE vapor on electrode surfaces [35] by understanding the thermal decomposition kinetics, and (c) investigating heterogeneous catalysis by examining the decomposition chemistry of different HE families on YSZ, LSCrO and Pt surfaces, thus enabling better anticipation of the response behavior.

Finally, the use of gas sensor arrays (increasing the number of selective sensors each targeting specific chemical groups comprising the HE) in combination with microfabrication would enable the design and construction of detector systems that would be low-cost, compact, low-power, and better positioned to reduce the high false positive rates endemic to today's widely used explosives detection technologies. For example, if a mixed potential ammonia sensor [36] is added to the current repertoire of sensors in the furnace, various explosives can be easily represented in a three-dimensional sensor space ( $\text{NO}_x$ ,  $\text{NH}_3$  and HC responses) with good resolution.

#### 4. Conclusions

In this article, selective and sensitive detection of trace amounts of explosives using electrochemical potentiometric gas sensors was demonstrated for the first time. An established sampling/concentrator system was coupled to the sensors as the front end.

The use of front-end technology to collect and concentrate the HE vapor emanating from areas and surfaces with trace HE contamination appears to make the intrinsically low vapor pressure of the HE samples less relevant as the strength of the measured response from the sensors did not scale with the samples' relative vapor pressure for equal quantities of HE. Hydrocarbon and nitrogen oxide(s) sensors were used to capture the electrochemical signature. The area under each sensor peak was calculated and found to be proportional to the amount of HE sample placed onto the hot wire and subsequently collected by the felt collector. Varying concentrations (1–3  $\mu\text{g}$ ) of PETN, TNT, and RDX were reliably detected. 250 ng of RDX was easily distinguished from the baseline response. Selective screening of explosives was shown possible by calculating the ratio of the HC peak area to the  $\text{NO}_x$  peak area for each explosive.

The significance of the proposed investigation is the ability to use multiple electrochemical gas sensors each tuned to basic chemical structures comprising almost all high explosive materials (e.g. nitro, amine, peroxide, and hydrocarbon groups) permitting the construction of detector systems with lower false positives than present day technologies taken together with the added benefit of greatly reduced detector purchase and operational costs. A great number of anticipated users (FBI, BATF&E, Army, etc.) can be provided with simple and inexpensive detectors for instant, on the spot screening of suspicious substances or trace detection from surface sampling. Subsequent mission will test a diverse palette of explosive compounds of different chemistries and to record the electrochemical HC and  $\text{NO}_x$  response for each explosive. The salient features of the explosive detection technology reported in the article are (a) a low-cost alternative conducive to mass manufacturing, (b) the reliable detection of explosives of different vapor pressures, and (c) the possibility of detecting a more diverse chemistry of explosive compounds.

#### Acknowledgement

P.K.S. and E.L.B. would like to thank the LANL Laboratory Directed Research and Development (LDRD) Office for the exploratory grant (#20100577ER).

#### Appendix A. Supplementary data

Supplementary data associated with this article can be found, in the online version, at doi:10.1016/j.jhazmat.2011.03.007.

#### References

- [1] Intelligence Reform and Terrorism Prevention Act of 2004, Public Law 108-458, Dec. 17, 2004.
- [2] L. Thiesen, D. Hannum, D.W. Murray, J.E. Parmeter, Survey of commercially available explosives detection technologies and equipment, Dept. Justice 208861 (2004) 1–96.
- [3] D.S. Moore, Recent advances in trace explosives detection instrumentation, *Sens. Imaging* 8 (2007) 9–38.
- [4] R.L. Woodfin, *Trace Chemical Sensing of Explosives*, John Wiley and Sons, 2007.
- [5] G.A. Eiceman, Z. Karpas, *Ion Mobility Spectrometry*, 2nd ed., Taylor and Francis Group, 2005.
- [6] R. Schulte-Ladbeck, U. Karst, Liquid chromatography–post-column photochemical conversion and electrochemical detection for discrimination of peroxide-based explosives, *Chromatographia* 57 (2003) S61–S65.
- [7] C. Yoder, ATF Specialist, Arson and Explosives Program Division, Bureau of Alcohol, Tobacco and Firearms.
- [8] S. Singh, Sensors—an effective approach for the detection of explosives, *J. Hazard. Mater.* 144 (2007) 15–28.
- [9] E. Capua, R. Cao, C.N. Sukenik, R. Naaman, Detection of triacetone triperoxide (TATP) with an array of sensors based on non-specific interactions, *Sens. Actuators B* 140 (2009) 122–127.
- [10] L. Senesac, T.G. Thundat, Nanosensors for trace explosive detection, *Mater. Today* 11 (2008) 28–36.
- [11] Y. Zhang, X. Ma, S. Zhang, C. Yang, Z. Ouyang, X. Zhang, Direct detection of explosives on solid surfaces by low temperature plasma desorption mass spectrometry, *Analyst* 134 (2009) 176–181.
- [12] M.S. Meaney, V.L. McGuffin, Luminescence-based methods for sensing and detection of explosives, *Anal. Bioanal. Chem.* 391 (2008) 2557–2576.
- [13] T. Caron, M. Guillemota, P. Montméata, F. Veignal, F. Perrautb, P. Prenéa, F. Serein-Spirauc, Ultra trace detection of explosives in air: development of a portable fluorescent detector, *Talanta* 81 (2010) 543.
- [14] A. Larsson, J. Angbrant, J. Ekeröth, P. Mansson, B. Liedberg, A novel biochip technology for detection of explosives—TNT: synthesis, characterization and application, *Sens. Actuators B* 113 (2006) 730–748.
- [15] J. Wang, Electrochemical sensing of explosives, *Electroanalysis* 19 (2007) 415–423.
- [16] B.J. Privett, J.H. Shin, M.H. Schoenfish, Electrochemical sensors, *Anal. Chem.* 82 (2010) 4723–4741.
- [17] K.L. Linker, F.J. Conrad, C.A. Custer, C.L. Rhykerd, Particle preconcentrator, US Patent #5854431 (1998).
- [18] K.L. Linker, F.A. Bouchier, D.W. Hannum, C.L. Rhykerd, Human portable preconcentrator system, US Patent #6523393 (2003).
- [19] K. Cizek, C. Prior, C. Thammakhet, M. Galik, K.L. Linker, R. Tsui, A. Cagan, J. Wake, J. La Belle, J. Wang, Integrated explosive preconcentrator and electrochemical detection system for 2,4,6-trinitrotoluene (TNT) vapor, *Anal. Chim. Acta* 661 (2010) 117–121.
- [20] E.L. Brosha, R. Mukundan, F.H. Garzon, YSZ based mixed potential sensors for the detection of explosives, *Electrochem. Solid State Lett.* 11 (2008) J92–J95.
- [21] F.H. Garzon, E.L. Brosha, R. Mukundan, Explosives detection sensor, US Patent #11110278.
- [22] G. Lu, N. Miura, N. Yamazoe, High temperature sensors for NO and  $\text{NO}_2$  based on stabilized zirconia and spinel-type oxide electrodes, *J. Mater. Chem.* 7 (1997) 1445–1449.
- [23] T. Hibino, A. Hashimoto, S. Sakimoto, M. Sano, Zirconia-based potentiometric sensors using metal-oxide electrodes for detection of hydrocarbons, *J. Electrochem. Soc.* 148 (2001) H1–H5.
- [24] D. Schönauer, K. Wiesner, M. Fleischer, R. Moos, Selective mixed potential ammonia exhaust gas sensor, *Sens. Actuators B* 140 (2009) 585–590.
- [25] R. Mukundan, E.L. Brosha, F.H. Garzon, A low temperature sensor for the detection of carbon monoxide in hydrogen, *Solid State Ionics* 175 (2004) 497–501.
- [26] R. Mukundan, E.L. Brosha, F.H. Garzon, Mixed potential hydrocarbon sensors based on a YSZ electrolyte and oxide electrodes, *J. Electrochem. Soc.* 150 (2003) H279–H284.
- [27] E.L. Brosha, R. Mukundan, R. Lujan, F.H. Garzon, Mixed potential  $\text{NO}_x$  sensors using thin film electrodes and electrolytes for stationary reciprocating engine type applications, *Sens. Actuators B* 119 (2006) 398–408.
- [28] F.H. Garzon, R. Mukundan, E.L. Brosha, Solid state mixed potential gas sensors: theory, experiments and challenges, *Solid State Ionics* 136–137 (2000) 633–638.
- [29] P.K. Sekhar, E.L. Brosha, R. Mukundan, W. Li, M.A. Nelson, P. Palanisamy, F.H. Garzon, Application of commercial automotive sensor manufacturing methods for  $\text{NO}_x/\text{NH}_3$  mixed potential sensors for on-board emissions control, *Sens. Actuators B* 144 (2010) 112–118.
- [30] F.H. Garzon, R. Mukundan, E.L. Brosha, Thin film mixed potential sensors, US Patent #7,264,700 (2007).
- [31] R. Mukundan, E.L. Brosha, F.H. Garzon, Electrodes for solid-state gas sensor, US Patent #6,605,202 (2003).

- [32] R. Mukundan, E.L. Brosha, F.H. Garzon, Tape-cast sensors and the method of making, US Patent #7575709 (2009).
- [33] R. Mukundan, K. Teranishi, E.L. Brosha, F.H. Garzon, Nitrogen oxide sensors based on yttria-stabilized zirconia electrolyte and oxide electrodes, *Electrochem. Solid State Lett.* 10 (2007) J26–J29.
- [34] J. Akhavan, *The Chemistry of Explosives*, 2nd ed., The Royal Society of Chemistry, 2004.
- [35] M. Mileham, J. Burk, P. Bhavsar, A.E. Steigman, M.P. Kramer, Stability and degradation processes of pentaerythritol tetranitrate (PETN) on metal oxide surfaces, *J. Energy Mater.* 26 (2008) 207–219.
- [36] R. Mukundan, E.L. Brosha, and F.H. Garzon, Ammonia and nitrogen oxide sensors, US Patent 11888736 (2007).